New level schemes with high-spin states of ^{105,107,109}Tc

Y. X. Luo,[1,2,3] J. O. Rasmussen,[3] J. H. Hamilton,[1] A. V. Ramayya,[1] J. K. Hwang,[1] S. J. Zhu,[1,4] P. M. Gore,[1] S. C. Wu,[5] I. Y. Lee,[3] P. Fallon,[3] T. N. Ginter,[3,6] G. M. Ter-Akopian,[7] A. V. Daniel,[7] M. A. Stoyer,[8] R. Donangelo,[9] and A. Gelberg[10]

[1]*Physics Department, Vanderbilt University, Nashville, Tennessee 37235, USA*
[2]*Institute of Modern Physics, Chinese Academy of Sciences, Lanzhou 730000, China*
[3]*Lawrence Berkeley National Laboratory, Berkeley, California 94720, USA*
[4]*Physics Department, Tsinghua University, Beijing 100084, China*
[5]*Department of Physics, National Tsing Hua University, Hsinchu, Taiwan*
[6]*National Superconducting Cyclotron Laboratory, Michigan State University, East Lansing, Michigan 48824, USA*
[7]*Flerov Laboratory for Nuclear Reactions, Joint Institute of Nuclear Research, Dubna, Russia*
[8]*Lawrence Livermore National Laboratory, Livermore, California 94550, USA*
[9]*Universidade Federal do Rio de Janeiro, CP 68528, RG Brazil*
[10]*Institut für Kernphysik, Universität zu Köln, 50937 Köln, Germany*

(Received 28 May 2004; published 19 October 2004)

New level schemes of odd-Z ^{105,107,109}Tc are proposed based on the ^{252}Cf spontaneous-fission-gamma data taken with Gammasphere in 2000. Bands of levels are considerably extended and expanded to show rich spectroscopic information. Spin/parity and configuration assignments are made based on determinations of multipolarities of low-lying transitions and the level analogies to the previously reported levels, and to those of the neighboring Rh isotopes. A non-yrast negative-parity band built on the $3/2^-[301]$ orbital is observed for the first time in ^{105}Tc. A positive-parity band built on the $1/2^+[431]$ intruder orbital originating from the $\pi(g_{7/2}/d_{5/2})$ subshells and having a strong deformation-driving effect is observed for the first time in ^{105}Tc, and assigned in ^{107}Tc. A positive-parity band built on the excited $11/2^+$ level, which has rather low excitation energy and predominantly decays into the $9/2^+$ level of the ground state band, provides evidence of triaxiality in ^{107,109}Tc, and probably also in ^{105}Tc. Rotational constants are calculated and discussed for the $K=1/2$ intruder bands using the Bohr-Mottelson formula. Level systematics are discussed in terms of the locations of proton Fermi levels and deformations. The band crossings of yrast positive-parity bands are observed, most likely related to $h_{11/2}$ neutron alignment. Triaxial-rotor-plus-particle model calculations performed with $\varepsilon=0.32$ and $\gamma=-22.5°$ on the prolate side of maximum triaxiality yielded the best reproduction of the excitation energies, signature splittings, and branching ratios of the positive-parity bands (except for the intruder bands) of these Tc isotopes. The significant discrepancies between the triaxial-rotor-plus-particle model calculations and experiment for the $K=1/2$ intruder bands in ^{105,107}Tc need further theoretical studies.

DOI: 10.1103/PhysRevC.70.044310 PACS number(s): 23.20.Lv, 21.10.Re, 25.85.Ca, 27.60.+j

I. INTRODUCTION

The intrinsic configurations, shape coexistence, and transitions in the neutron-rich nuclei with $Z\sim40$, $N>58$ have drawn much attention. Proton orbitals originating from the $\pi g_{9/2}$ subshell closest to the Fermi level are affected in special ways by triaxial nuclear shapes (β_2,γ) [1]. Neutron states from the $\nu h_{11/2}$ subshell strongly drive nuclei in this region to prolate deformation, since the neutron Fermi level is below or near the bottom of the $\nu h_{11/2}$ subshell. A large prolate-deformation driving effect is also expected for the intruder $\pi 1/2^+[431]$ orbital originating from the $\pi(g_{7/2}/d_{5/2})$ subshells, which are located above the $Z=50$ major shell gap. Shape coexistence and transitions in the even-even nuclei in this region have been intensively studied [2,3]. In contrast to the sharp shape transitions and coexistence observed in nuclei of $Z\leqslant40$, the appearance of triaxiality and soft shape transitions were found in nuclei of $Z>40$ [4].

Not much is known about the odd-Z neutron-rich nuclei in this region. Because of the deformations driven by $N>60$ neutrons, various proton subshells are near the Fermi levels and may play a role in the odd-Z nuclei. Rotational bands built on $\pi g_{9/2}$, $\pi p_{1/2}$, and $\pi(g_{7/2}/d_{5/2})$ subshells have been observed in ^{107,109}Rh [5], and ^{111,113}Rh with $Z=45$ [6,7]. In our previous work on Rh isotopes, calculations with a triaxial-rotor-plus-quasiparticle model give a reasonable fit to excitation energies and signature splitting of the $7/2^+$ $\pi g_{9/2}$ bands, as well as collective yrare bands and to transition probabilities at near-maximum triaxiality with $\gamma\cong-28°$ for ^{111,113}Rh [7]. Yrare bands built on the excited $11/2^+$ states also provided evidence of triaxiality. Intruder $1/2^+[431]$ bands are identified in ^{111,113}Rh [7] but there are discrepancies with theory.

In our work investigation of the odd-Z isotopes ^{105,107,109}Tc with $Z=43$, which are odd-Z neighbors of Rh with $Z=45$, are carried out. Like the neutron-rich isotopes ^{111,113}Rh ($Z=45$) [6,7], ^{105,107,109}Tc are several protons below the 50-proton closed shell and midway in the 50–82 neutron shell, a region of nuclei characterized by differing deformations, including γ softness or rigid triaxiality. In view of the difference of proton number by two, the Tc isotopes are ex-

pected to exhibit some differences in structure and shapes from the Rh isotopes.

Low-lying transitions of Tc isotopes were obtained from β-decay work [8]. The lowest transitions of ^{105}Tc from β decay of ^{105}Mo and of ^{107}Tc from β decay of ^{107}Mo were reported [8]. However, nothing has been known for the low-lying states of ^{109}Tc from β decay of ^{109}Mo. The first high-spin level schemes of ^{105,107,109}Tc were proposed by Hwang *et al.* [9] of our collaboration using spontaneous fission of ^{252}Cf at Gammasphere. High-spin states in ^{101}Tc were studied by Hoellinger *et al.* using fusion-fission reactions at EUROGAM2 [10]. Similar studies for ^{97}Tc and ^{99}Tc were reported by Aslan *et al.* [11] and by Crowe *et al.* [12], respectively. Recently, Bauchet *et al.* [13] reported on the high-spin states of ^{103}Tc also using fusion-fission reactions at Euroball III.

In this paper we propose new level schemes of ^{105,107,109}Tc based on the compressed and less-compressed cubes of our 1995 and 2000 high-statistics fission-gamma data taken at Gammasphere. Spin/parity and configurations involved in ^{105,107,109}Tc are assigned. Level-structure systematics of the Tc isotopes are discussed. Rigid-triaxial-rotor-plus-particle model calculations for the Tc isotopes are performed and compared with the data. This comparison favors a triaxial shape, $\varepsilon_2 = 0.32$, and $\gamma = -22.5°$ for the main positive-parity bands in ^{107}Tc.

II. EXPERIMENT AND DATA ANALYSIS

It has been shown that the combination of spontaneous- or induced-fission reactions with multi-gamma-detector arrays provide a powerful method for the population and identification of energy levels of neutron-rich nuclei [3]. For two runs, each taking two weeks in 2000, a ^{252}Cf source of 62 μCi, sandwiched between two 10 mg/cm^2 Fe foils, was placed in an 8-cm polyethylene ball centered in the Gammasphere, which had 102 active Compton-suppressed Ge detectors. Over 5.7×10^{11} triple and higher-fold events were accumulated. This number of events considerably exceeded those in our 1995 run, and the efficiency for low-energy ($<$100 keV) gamma rays was considerably improved over that in 1995. The high statistics and high quality data make it possible to observe the weakly populated bands and to extend bands to higher spins and excitations than could be identified from our 1995 data alone.

The coincidence data analysis used the RADWARE software package [14]. Double-gating on the known transitions and cross-checking by gating on Tc transitions and its fission partner Cs transitions, new transitions were identified, and bands of ^{105,107,109}Tc were extended and expanded. We paid close attention to the corresponding partner transitions, coincidence relationships and balance of relative intensities. Background subtractions were carefully made in the gated spectra by shifting gates off the peaks. The adopted transition energies and relative intensities were determined with special care by peak-fitting using the gf3 program, and the former were weighted-averaged over several gated spectra.

We have used first the regular RADWARE cube with its standard compression of 8192 channels over $\sim$5 MeV. We have rechecked with a special version recently supplied by Dr. Radford, which has about a third less compression, and consequently requires more memory on hard disk. The less-compressed cube was found to be useful in clarifications of ambiguities related to peak overlapping, in identifications of weak transitions and bands smeared by contaminating strong transitions in the coincidence spectra, and in least-squares fitting of transition energies with higher precisions.

Figures 1(a), 1(b), and 1(c) shows a typical double-gated, triple-coincidence gamma spectrum for ^{105}Tc, ^{107}Tc, and ^{109}Tc, respectively, based on the less-compressed cube. See details in the figure caption.

III. NEW LEVEL SCHEMES AND SPIN/PARITY/ CONFIGURATION ASSIGNMENTS

The new level schemes of ^{105,107,109}Tc based on our high statistics ^{252}Cf fission data are displayed in Figs. 2, 3, and 4, respectively. The numbering of bands follows that used in Ref. [7]. Tables I, II, and III show energies, relative intensities, initial levels, and half-lives (if any) determined for all the transitions of ^{105}Tc, ^{107}Tc, and ^{109}Tc, respectively. There are several levels with lifetimes determined in Ref. [15] by Rücker, and these half-lives are noted in Table I, as well as in the Table of Isotopes [8].

We have put two decimal places on our energies in column 1 in order to facilitate testing sum relationships in the decay scheme and for determining signature splitting. We do not believe the absolute transition energies are accurate to better than 0.1 keV. We list the statistical standard deviations rounded to nearest 0.01 keV, as returned by the gf3 fitting program on the expanded RADWARE cube, but we state that systematic standard deviation is about 0.1 keV. The comparison with work of others as shown in the tables bears this out.

A. ^{105}Tc

The level scheme of ^{105}Tc is considerably extended and expanded (see Fig. 2). The $\alpha = -1/2$ signature branch of band 1 in ^{105}Tc reported in Ref. [9] is extended from the 1177.7-keV $(15/2^+)$ level, up to a 3348.2-keV $(27/2^+)$ level (so the band crossing is now observed, see below), and the $\alpha = +1/2$ branch from the 2118.9-keV $(21/2^+)$ up to the 3716.2-keV $(29/2^+)$ level. New cross-linking transitions of 495.1 keV, 249.8 keV, 503.3 keV, 309.7 keV, and 416.3 keV are observed among the newly identified levels of band 1. A new band 5 reaching up to 2759.3 keV $(23/2^+)$ for its $\alpha = -1/2$ member and to 1396.9 keV $(13/2^+)$ for its $\alpha = +1/2$ branch was observed for the first time in our work. It was very difficult to identify band 5 when using the standard compressed RADWARE cube because of serious peak overlapping (for example, the 507.3-keV transition in band 5 lies next to the 511-keV transition) and weak populations smeared by stronger contaminating peaks. However, this band clearly shows up when using the less-compressed new RADWARE cube for analysis. The band is found to be built on the low-lying 304.0-keV $(3/2^+)$, 322.2-keV $(1/2^+)$, 530.2-keV $(5/2^+)$, and 491.8-keV $(7/2^+)$ levels, which are also reported by beta-decay work [8]. Another new band, band 6,

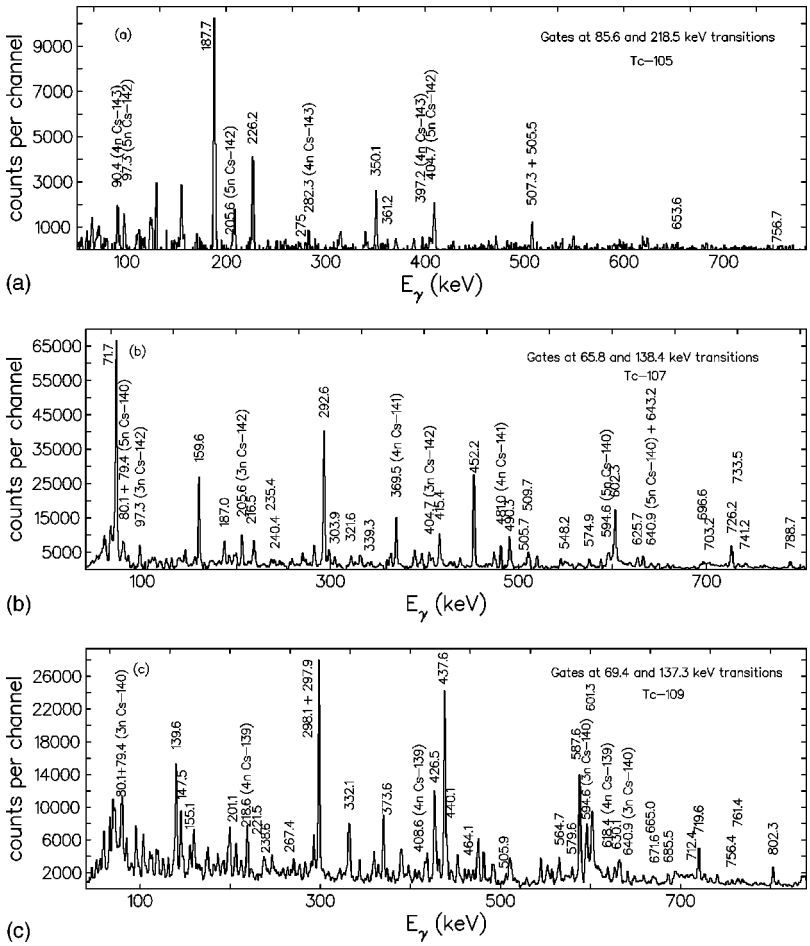

FIG. 1. (a) A double-gated, triple-coincidence γ spectrum for ^{105}Tc analysis. The weakly populated and smeared intruder band, band 5, in ^{105}Tc is identified for the first time using the less-compressed cube. All the available fission partner transitions are seen; see text. (b) A double-gated, triple-coincidence γ spectrum for ^{107}Tc analysis; see text. (c) A double-gated, triple-coincidence γ spectrum for ^{109}Tc analysis; see text.

consisting of only two levels, is observed, with one of the transitions, 531.1 keV, also reported by decay studies [8].

The $\alpha=-1/2$ branch of band 9 is extended from the 1236.2-keV $(15/2^-)$ up to 3252.0-keV $(27/2^-)$, and the $\alpha=+1/2$ branch from the 951.6-keV $(13/2^-)$ up to 2283.0-keV $(21/2^-)$ level. New 284.5-keV, 340.6-keV, 321.9-keV, 384.4-keV, and 347.7-keV transitions are found to cross-link the new levels of band 9.

A new band 10 is observed based on the ground state $3/2^-$, which confirms the 346.0-keV $7/2^-$ level and the 147.7-keV and 198.3-keV transitions reported by decay measurements [8]. Band 10 was extended up to a 838.8-keV $(11/2^-)$ level by observing a new 493.0-keV transition. The identification of band 10 starting from the ground state $3/2^-$ indicates that differing from the previous reports, band 9 has the $5/2^-$ state as the band head, the band head of band 10 is $3/2^-$, and the two bands have different configurations (see discussion below). The lower part in the level scheme of ^{105}Tc (see Fig. 2) shows the transitions emitted from the levels identified in our prompt-fission-gamma work and reported in beta-decay studies [8], but not identifiable directly in our fission data.

The assignment of $3/2^-$ to ground state of ^{105}Tc was given in Ref. [8]. The spin/parity assignments for the low-lying levels of ^{105}Tc were based on the determinations of multipolarities of the lowest-lying transitions [8,9]: 85.6 keV $E1$, 64.5 keV $M1$, 129.2 keV $M1$, 76.8 keV $M1$, 160.5 keV $M1$, and 204.1 keV $M1$. This then led to the assignments of the following low-lying levels: 85.6 keV $5/2^+$, 150.1 keV $7/2^+$, 279.3 keV $9/2^+$, 76.8 keV $5/2^-$, 237.3 keV $7/2^-$, and 441.3 keV $9/2^-$. In our work, the total internal conversion coefficients (ICC) of some low-lying transitions were determined based on the intensity balance corrected for the total ICC as well as detection efficiency. Gating at the 157.0- and 623.4-keV transitions, the ICC of the 129.2-keV transition was derived to be 0.26(9) based on the intensity balance between 314.2- and 129.2-keV transitions. Then gating at the 471.1/623.4-keV transitions and 314.2/157.0-keV transitions, the ICC of the 85.6-keV and 64.5-keV transitions are deduced to be 0.22(8) and 1.13(10), respectively, using the above-determined ICC of the 129.2-keV transition [0.26(9)]. The derived ICC were compared to Hager-Seltzer theoretical values to derive the multipolarities: 85.6-keV transition $E1$, 64.5-keV transition $M1$ $(+E2)$, 129.2-keV transition $M1+E2$, the former two being also reported in Ref. [8]. Using the same method, gating on the 129.2- and 623.4-keV transitions, the ICC value of the 157.0-keV transition is determined to be 0.09(4), implying a $M1$ $(+E2)$ transition with a predominant component of $M1$. The determined ICC values and derived multipolarities of low-lying transitions in ^{105}Tc are indicated in Table IV, which supports the spin/parity assignments for the lowest-lying levels of ^{105}Tc (see Fig. 2).

The spin/parity assignments of the extended parts of bands 1 and 9 are based on reasonable assumptions of rota-

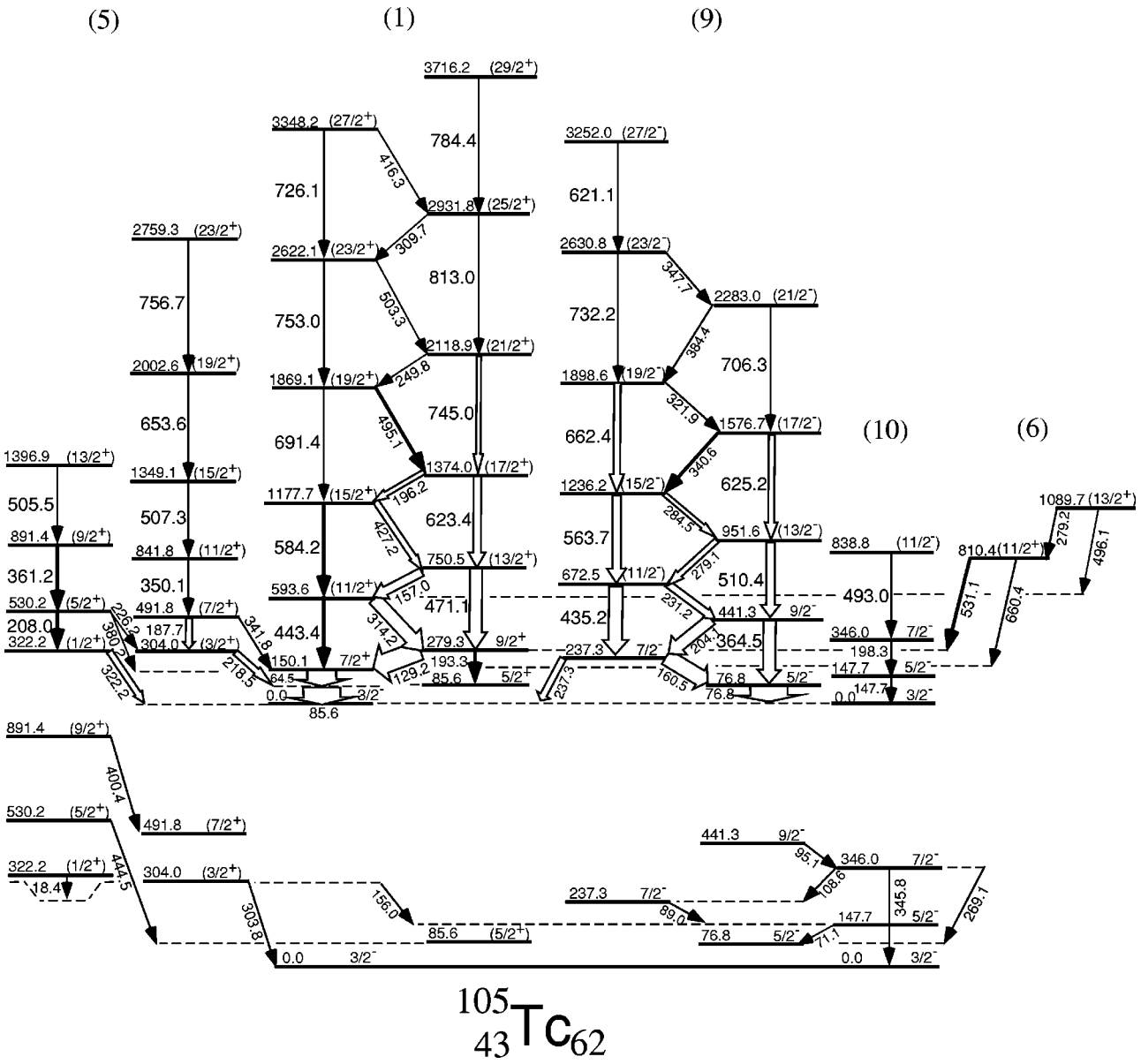

FIG. 2. New level scheme of ^{105}Tc proposed in this work. The widths of the arrows are roughly representative of the relative intensities of the transitions. Refer to Table I for measured values.

tional character and analogous level patterns to those reported in Ref. [9] and to ^{107,109,111,113}Rh [5–7]. For the new band 10, we felt it reasonable to assign $11/2^-$ to the 838.8-keV level and the E2 multipolarity to the newly observed 493.0-keV transition. In the new band 5, similar to those of ^{107,111,113}Rh [5–7], we follow the same assignments with $7/2^+$ assigned to the 491.8-keV level, so that band 5 also consists of two signature partners, as was observed in ^{111,113}Rh [7]. Band 6 is assumed to be built on the excited $11/2^+$ level, an assignment which is supported by the level systematics and decay patterns of the corresponding bands in ^{107,109}Tc and those in ^{107,109,111,113}Rh [7] (see below).

The band assignments of asymptotic Nilsson quantum numbers $\Omega^\pi[Nn_z\Lambda]$ is attempted here, mainly for the purpose of labeling, since the triaxiality of most of the bands will bring about considerable configuration mixing. In a later section we apply a triaxial-rotor-plus-particle model to make a more sophisticated analysis. The ground $3/2^-$ state was assigned $1/2^-[301]$ orbital [9]. The configuration $7/2^+[413]$ was assigned to the yrast positive-parity band 1, though our model calculations below show nearly equal admixtures of $7/2^+[413]$ and $5/2^+[422]$ in most levels [9]. The observation of the new non-yrast, negative-parity band 10 built on the $3/2^-$ ground state suggests a new interpretation for the yrast negative-parity band 9 differing from that given in Ref. [9]. Assuming a prolate deformation $\beta \sim 0.25$, $5/2^-[303]$ is assigned to band 9, and $3/2^-[301]$ to new band 10. Band 6 is considered a $K+2$ satellite band originating from the $7/2^+[413]$ band (see discussion below for ^{107}Tc).

Of particular interest is the interpretation of the new band 5. Lhersonneau *et al.* [16] measured lifetimes of the band heads in the analogous bands in ^{109,111}Rh. These data imply strong retardations for the $E2$ transitions to the ground $7/2^+$ states and suggest that the bands originate from $\pi 1/2^+[431]$

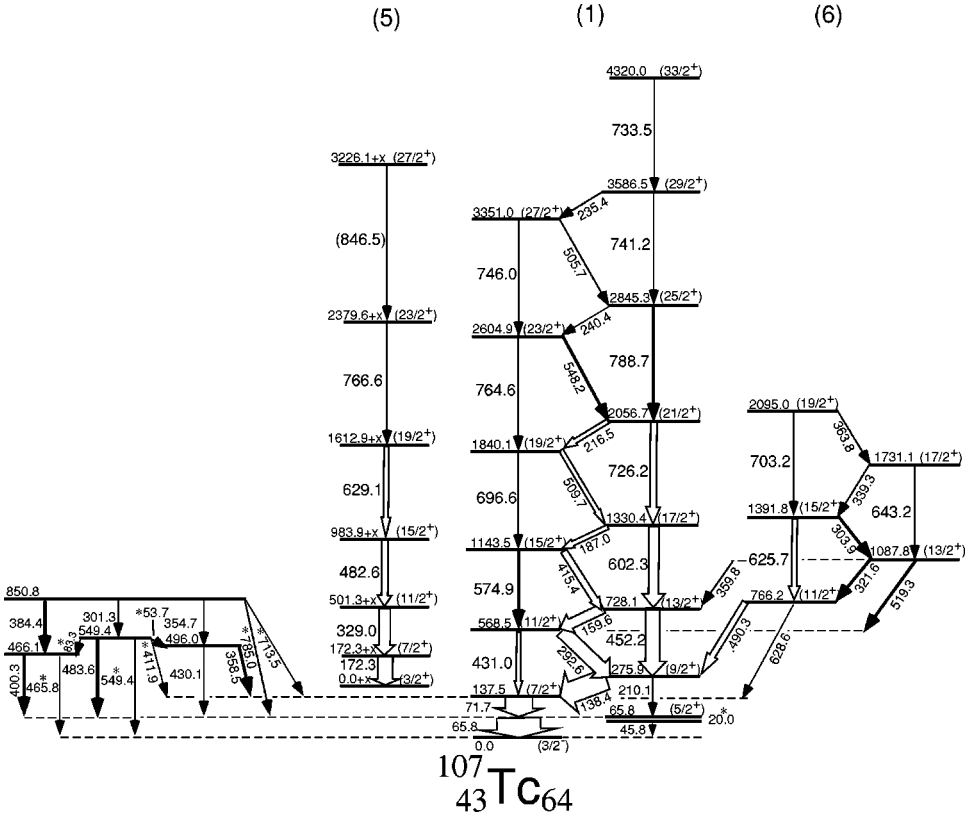

FIG. 3. New level scheme of ^{107}Tc proposed in this work. The widths of the arrows are roughly representative of the relative intensities of the transitions. Refer to Table II for measured values.

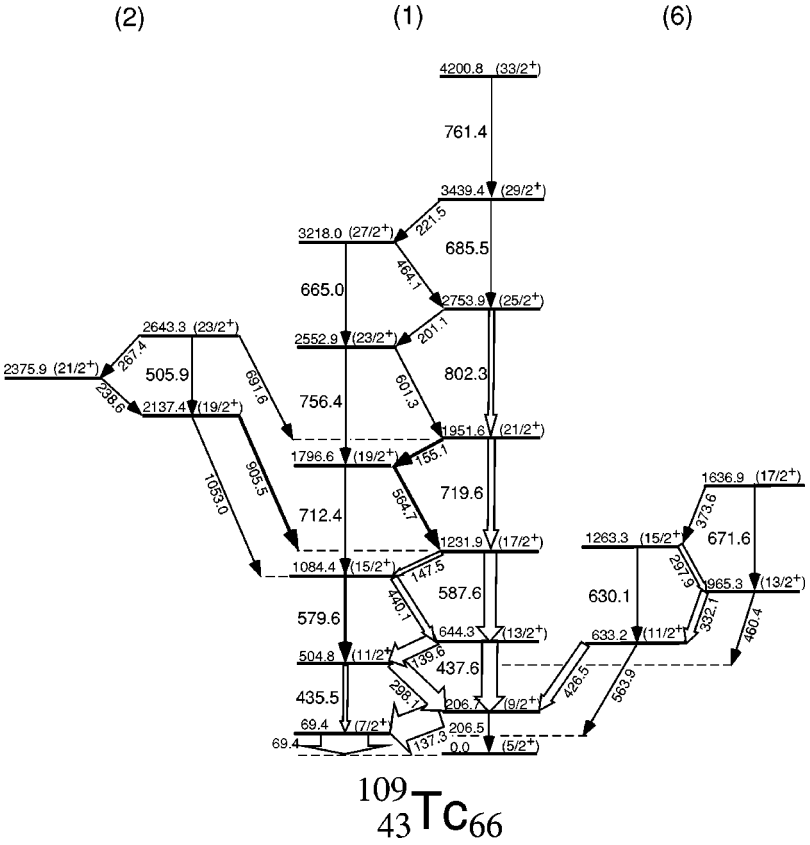

FIG. 4. New level scheme of ^{109}Tc proposed in this work. The widths of the arrows are roughly representative of the relative intensities of the transitions. Refer to Table III for measured values.

TABLE I. Energies and relative intensities of the transitions observed in ^{105}Tc.

E_γ (keV)	Statistical std. dev. σ (keV)	Relative intensities[a]	E_γ[9] (keV)	E_γ^β[8] (keV)	Initial level (keV)	Half-life (ns)
				18.4(1)	322.2	9.9(11)
64.49	0.01	72.5	64.1	64.1(2)	150.1	
				71.1(2)	147.7	
76.81	0.01	~110	76.5	76.5(1)	76.8	0.93(4)
85.60	0.01	100.0	85.4	85.4(1)	85.6	20.8(6)
		{5.3}		89.0(1)	237.3	
				95.1(2)	441.3	
				108.6(2)	346.0	-
129.19	0.01	44.0	129	129.0(1)	279.3	
147.72	0.01		147.8	147.8(1)	147.7	
		{0.2}		156.0(2)	304.0	
157.04	0.01	6.3	157.2		750.5	
160.47	0.01	33.1	160.5	160.5(1)	237.3	
187.68	0.01	3.1		187.7(2)	491.8	
193.30	0.10	1.4		193.2(2)	279.3	
196.20	0.02	2.6	196.2		1374.0	
198.34	0.03		197.9	197.9(1)	346.0	
204.06	0.01	13.9	204.2	203.9(1)	441.3	-
208.0	0.1	2.1		207.8(2)	530.2	0.175(6)
218.48	0.01	5.3		218.4(1)	304.0	6.8(10)
226.18	0.04	1.3		226.3(2)	530.2	0.175(6)
231.24	0.01	5.6	231.5		672.5	
237.33	0.07	3.6	236.9	236.9(5)	237.3	-
249.78	0.04	0.9			2118.9	
				269.1(1)	346.0	
279.14	0.02	3.0	278.3		951.6	
279.24	0.10	0.3			1089.7	
284.48	0.05	2.6			1236.2	
		{2.8}		303.8(1)	304.0	
309.72	0.08	0.3			2931.8	
314.34	0.01	14.8	314.4		593.6	
321.94	0.06	1.7			1898.6	
322.19	0.06	5.1		322.2(1)	322.2	
340.56	0.02	2.4			1576.7	
341.84	0.06	{1.1}		341.8(2)	491.8	
			345.9	345.8(3)	346.0	
347.74	0.25	0.6			2630.8	
350.05	0.01	1.7			841.8	
361.19	0.02	1.2		361.5	891.5	
364.50	0.01	13.9	364.7	364.3(1)	441.3	
380.20	0.02			380.4(2)	530.2	0.175(6)
384.40	0.04	1.2			2283.0	
416.3	0.1				3348.2	
427.16	0.02	4.3	427.5		1177.7	
435.18	0.01	14.1	435.7		672.5	
443.35	0.03	1.7	443.4		593.6	
				444.5(2)	530.2	0.175(6)
471.07	0.01	12.3	471.2		750.5	

TABLE I. (*Continued.*)

E_γ (keV)	Statistical std. dev. σ (keV)	Relative intensities[a]	E_γ[9] (keV)	E_γ[8] (keV)	Initial level (keV)	Half-life (ns)
493.04	0.04				838.8	
495.11	0.02	1.4			1869.1	
496.13	0.11				1089.7	
503.27	0.07	0.5			2622.1	
505.46	0.07	0.3			1396.9	
507.28	0.01	0.6			1349.1	
510.4	0.1				951.6	
531.14	0.02	1.8			810.1	
563.69	0.01	7.2	563.7		1236.1	
584.19	0.03	1.2	584.2		1177.6	
621.20	0.10	0.4			3252.0	
623.43	0.01	5.5	623.5		1374.0	
625.18	0.05	4.6			1576.7	
653.54	0.02	0.4			2002.6	
660.42	0.11	0.2			810.4	
662.41	0.02	4.3			1898.6	
691.35	0.07	0.8			1869.1	
706.25	0.13	1.4			2283.0	
726.05	0.10	0.1			3348.2	
732.24	0.05	1.6			2630.8	
744.95	0.14	2.8	744.7		2118.9	
753.01	0.11	0.3			2622.1	
756.68	0.02				2759.3	
784.4	0.1	0.1			3716.2	
812.99	0.17	0.8			2931.8	

[a]The relative intensities given in curly brackets are those determined by β decay measurements [8].

from the major shell above, probably with a different shape from the ground band. With the above interpretations, the analogous new positive-parity band 5 is interpreted as from an intruder orbital $\pi 1/2^+[431]$ originating from the $\pi(g_{7/2}/d_{5/2})$ subshells, which exert a strong prolate-deformation-driving effect. It is also of interest to note the "anomalous" level spacing characteristic of $K=1/2$ bands in the level sequence of the newly observed $\pi 1/2^+[431]$ rotational band. Here the $3/2^+$ level lies just below the $1/2^+$ level, and the $7/2^+$ level below the $5/2^+$ level, forming two doublets. This irregular level sequence was also observed in ^{107}Rh [5] and ^{111,113}Rh [7], which was explained by the decoupling parameter, a, between -1 and -2 (also see Sec. IV).

Band 6, built on the excited $11/2^+$ state with a strong decay-out transition of 531.1 keV $(11/2^+)_{\rm exc}\rightarrow 9/2^+_1$ and a very weak one, 660.4 keV $(11/2^+)_{\rm exc}\rightarrow 7/2^+_1$, provides evidence of triaxiality (see discussions below for ^{107,109}Tc). However, no further information could be obtained since only two levels are observed in this band. There are several levels with lifetimes by Rücker [15], and these half-lives are noted in Table I.

B. ^{107}Tc

The $\alpha=-1/2$ signature branch of band 1 in ^{107}Tc reported in Ref. [9] is extended from 1840.1 keV $(19/2^+)$ up to 3351.0 keV $(27/2^+)$ (so the band crossing is now observed, see below), the $\alpha=+1/2$ branch from 3586.5 keV $(29/2^+)$ up to 4320.0 keV $(33/2^+)$. The dashed cross-linking 216.5-keV transition given in Ref. [9] is confirmed, and new cross-linking transitions in band 1, namely, 548.2-, 240.4-, 505.7-, and 235.4-keV transitions, are observed in our work.

The transition of 766.0 keV in band 5 tentatively given in Ref. [9] is confirmed (measured to be 766.6 keV), and the band is tentatively extended by one level. This band is very similar to the band 5 of ^{105}Tc except that in ^{107}Tc no transitions connecting band 5 to other bands or the ground state are observed. Either the linking transitions are too low in energy for us to observe with any efficiency or the $3/2^+$ band head decays out with a lifetime long compared to the ~ 1 μs resolving time of our data set. So the excitation energies of band 5 given in the level scheme are not absolute values.

The 850.8-, 549.4-, 496.0-, and 466.1-keV levels reported in the decay measurements [8] are identified in our work, and they form several new sequences observed for the first time in ^{107}Tc using fission data. The transitions with asterisks in the level scheme (Fig. 3) are those reported in Ref. [8] but not identified with fission data.

Two new levels at 1731.1 keV $(17/2^+)$ and 2095.0 keV $(19/2^+)$ are added to band 6. New transitions, 339.3 and 363.8 keV, are observed between the two signature partners of band 6.

TABLE II. Energies and relative intensities of the transitions observed in ^{107}Tc.

E_γ (keV)	Statistical std. dev. σ (keV)	Relative intensities[a]	E_γ[9] (keV)	E_γ^β[8] (keV)	Initial level (keV)	Half-life (ns)
				20.0	65.8	
45.83	0.03	{78.8}		45.6	45.8	
				53.7	549.4	
65.77	0.01	100	65.7	65.7	65.8	184(3)
71.72	0.01	78.8	71.7	71.7	137.5	
				83.3	549.4	
138.40	0.01	61.5	138.6		275.9	
159.58	0.01	15.1	160.1		728.1	
172.34	0.01	18.8	172.6		172.3+x	
187.01	0.01	4.9	187.4		1330.4	
210.1	0.1	0.3			275.9	
216.54	0.04	4.1	(217.2)		2056.7	
235.39	0.12				3586.5	
240.41	0.04	1			2845.3	
292.58	0.01	20.6	292.8		568.5	
301.42	0.03	{2.4}		301.3	850.8	
303.93	0.02	1.6	304.1		1391.8	
321.56	0.01	2.1	321.9		1087.8	
329.00	0.01	14.1	329.1		501.3+x	
339.28	0.03	0.6			1731.1	
354.74	0.04	0.8	354.8	354.8	850.8	
358.51	0.04	7.2	358.9	358.5	496.0	
359.86	0.09		359.6		1087.8	
363.82	0.07	0.3			2095.0	
384.37	0.06	{7.2}		384.4	850.8	
400.38	0.05	{7.2}		400.3	466.1	
				411.9	549.4	
415.40	0.01	6.3	415.3		1143.5	
430.14	0.03	{3.4}		430.1	496.0	
430.96	0.01	3.1	431.3		568.5	
452.23	0.01	20.5	452.4		728.1	
		{0.2}		465.8	466.1	
482.55	0.01	8.9	482.7		983.9+x	
483.64	0.02	{7.2}		483.6	549.4	
490.29	0.01	6.6	490.3		766.2	
505.70	0.07	0.5			3351.0	
509.69	0.02	4.6	509.5		1840.1	
519.34	0.02	2.8			1087.8	
548.23	0.03	1.2			2604.9	
		{1.4}		549.4	549.4	
574.92	0.02	1.6	574.9		1143.5	
602.28	0.01	14.9	602.4		1330.4	
625.68	0.01	4.3	625.8		1391.8	
628.56	0.02	0.9			766.2	
629.05	0.02	4.2	629.1		1612.9+x	
643.15	0.06	0.2			1731.1	
696.59	0.02	0.9	696.9		1840.1	
703.16	0.08	0.9			2095.0	

TABLE II. (*Continued.*)

E_γ (keV)	Statistical std. dev. σ (keV)	Relative intensities[a]	E_γ[9] (keV)	E_γ^β[8] (keV)	Initial level (keV)	Half-life (ns)
		{0.3}		713.5	850.8	
726.24	0.01	7.9	726.7		2056.7	
733.46	0.09	0.2			4320.0	
741.23	0.06	0.9	742		3586.5	
746.01	0.12	0.1			3351.0	
764.58	0.04	0.3			2604.9	
766.63	0.06	2.0			2379.6+x	
		{3.4}		785.0	850.8	
788.74	0.03	1.8	789.5		2845.3	
846.5	0.1				3226.1+x	

[a]The relative intensities given in curly brackets are those determined by β decay measurements [8].

The spin/parity assignments of the bands were based on the determinations of multipolarities of the lowest-lying transitions, on the assumption of rotational sequence and on the level patterns analogous to reported levels and neighboring Rh isotopes. In Ref. [8] the lowest-lying 65.8- and 71.7-keV transitions were reported by Ohm *et al.* [8] to have $M1+E2$ and D (dipole) character, respectively. Their results of ICC determinations and the deduced multipolarities are indicated in Table IV. In Table IV we have substituted the slightly different theoretical values calculated from the interpolation program on the website of the National Nuclear Data Center at Brookhaven National Laboratory.

The determinations of total ICC of the 65.8- and 71.7-keV transitions in our work, and consequently the deduced multipolarities, differ from those reported by Ohm *et al.* [8]. By gating on 159.3-keV and 602.3-keV transitions the total ICC of the 138.4-keV transition was determined to be 0.16(8) from intensity balances between the 292.6-keV and 138.4-keV transitions corrected for ICC, as mentioned above for ^{105}Tc. Then by gating above the 138.4-keV transition (with either the 292.6-keV or 452.5-keV transition always involved) on several pairs of transitions, the total ICC deductions for multipolarities of the 65.8- and 71.7-keV transitions are determined to be <1.06 and 0.65(8) (see Table IV), respectively. A 45.6-keV ground transition and a 20-keV transition between the 65.8-keV level and ground state were reported in decay work [8]. The 20-keV transition, however, was not observed in our work because the detection cutoff was $\sim$35 keV, so only an upper limit of the total ICC of the 65.8-keV transition was given. In comparison with the theoretical values of the ICC (see Table IV) the multipolarities of the 65.8-, 71.7-, and 138.4-keV transitions were determined to be $E1$, pure $M1$, and $M1(+E2)$, respectively. The one-page report of Ohm *et al.* [8] does not give sufficiently specific information to decide how they might overestimate the total ICC of the 65.8-keV transition. If the experimental total ICC of the 65.8-keV transition is actually greater than the theoretical $E1$ value, it may be that there is some $M2$ admixture or it is another case of anomalous $E1$ conversion coefficients. In a similar way, gating on the 138.4- and 602.3-keV transitions, the total ICC of the 159.6-keV transition is determined to be 0.09(2), implying $M1(+E2)$ character with predominant component of $M1$ (see Table IV).

There are no spin/parity assignments of low-lying levels in Ref. [8] for ^{107}Tc. Now, with $3/2^-$ being assigned to the ground state following the assignment for ^{105}Tc, $5/2^+$ is assigned to the 65.8-keV level based on the above determinations of multipolarities of 65.8- and of 71.7-keV transitions. It can be seen that now the yrast $5/2^+$, $7/2^+$ levels of ^{105,107}Tc follow the same level pattern as seen in ^{103,105}Tc and smooth level evolution is also seen in the isotopic chain (also see the next section). The smooth level systematics and decay pattern support the above determinations of multipolarities of the 65.8- and 71.7-keV transitions and the spin/parity assignments for the lowest levels of ^{107}Tc.

The assignments of spin/parity for the extended parts of band 1 are based on the rotational sequence and analogous level pattern. The spin/parity assignments for bands 5 and 6 are also based on the similarity of level patterns with those of ^{105}Tc and ^{107,109,111,113}Rh [5–7].

Positive-parity band 1 was assigned a $7/2^+[413]$ configuration. The negative-parity band 10, interpreted as $3/2^-[301]$ in ^{105}Tc, is not observed in ^{107}Tc. Band 6, built on the excited $11/2^+$ state, has rather low excitation energy and deexcites to the $g_{9/2}$ band (predominantly feeding the $9/2^+$ and very weakly the $7/2^+$ states) as seen in ^{107,109,111,113}Rh. For the rhodiums this low-lying $11/2^+$ band was interpreted in our previous paper as evidence of triaxiality [7]. The quenching of the $11/2_{\rm exc}\rightarrow 7/2_1$ transition was explained by examining the wave functions. The main core component in the wave functions of both the initial and final states is the first 2^+ core state; thus the $E2$ transition strength is mainly dictated by the diagonal $E2$ reduced matrix element, which vanishes for $\gamma=-30°$. However, the main core component of the $9/2_1$ state is the 0^+ state of the core, resulting in a large $B(E2;11/2_{\rm exc}\rightarrow 9/2_1)$. Based on the analogies of level structure and decay patterns, band 6, observed in ^{107}Tc and in ^{105}Tc, provides the strong evidence of triaxiality in these Tc isotopes. The analogous $11/2^+$ bands in ^{107,109}Rh were also interpreted as coupling of the $7/2^+[413]$ and the 2^+ γ phonon of the core by Venkova *et al.* [5], but we think the phonon interpretation is misleading and should be superseded by the fixed-shape triaxial-rotor model used in our present work. For one thing the $11/2^+$ band head is too low in energy to be

TABLE III. Energies and relative intensities observed in ^{109}Tc.

E_γ (keV)	Standard deviations σ (keV)	Relative intensities	E_γ [9] (keV)	Initial level (keV)
69.43	0.01		69.1	69.3
137.26	0.01	100	137.6	206.6
139.63	0.01	23.3	139.6	644.3
147.49	0.01	2.9	147.7	1231.9
155.13	0.01	1.6		1951.5
201.1	0.1	0.4		2753.9
206.54	0.11	<1.5		206.6
221.49	0.21			3439.4
238.58	0.09	0.4		2376.2
267.41	0.11	0.2		2643.6
297.91	0.01	3.6		1262.9
298.08	0.01	28.0	298.3	504.7
332.09	0.01	7.8	332	964.9
373.62	0.07	0.3		1635.9
426.53	0.01	9.9	426.6	633.1
435.51	0.01	2.8	435.9	504.7
437.58	0.01	22.4	437.9	644.3
440.12	0.02	5.7	440	1084.3
460.44	0.08	1.2		964.9
464.10	0.09			3217.9
505.89	0.06	0.5		2643.6
563.9	0.1	0.9		633.1
564.70	0.01	1.9		1796.4
579.56	0.02	1.8	579.6	1084.3
587.59	0.01	17.9	587.7	1231.9
601.33	0.21	0.8		2552.6
630.08	0.02	2.1		1262.9
665.01	0.20	0.3		3217.9
671.57	0.04	0.7		1635.9
685.46	0.04	1.6	685.6	3439.4
691.55	0.15	0.2		2643.6
712.43	0.05	1.1		1796.4
719.57	0.01	7.9	719.8	1951.5
756.40	0.11	0.4		2552.6
761.37	0.06	0.4		4201.1
802.33	0.02	2.8	802.6	2753.9
905.51	0.09	1.4		2137.3
1053.0	0.5			2137.3

a gamma-phonon band, and the near vanishing of the $E2$ transition from $11/2^+$ band head to $7/2^+$ band head of band 1 is uncharacteristic of a gamma vibration and is a signature of substantial triaxiality. If one were to consider gamma vibrations, they should be fluctuations about a triaxial shape. Our model calculations do not incorporate such a refinement, and we feel it is not important for the lower-lying bands considered here.

We have struggled to come up with a term denoting band 6, which is clearly in the collective family of band 1. We suggest the term "$K+2$ satellite band." In our paper on the analogous odd-A rhodium isotopes we have also clearly seen what we would call a "$K-2$ satellite band." That is, there is a low-lying band with band head $3/2^+$ that decays by enhanced $E2$ transitions to band 1. That such a $3/2^+$ band is not observed in the Tc isotopes experimentally and is not evident in the theory may be due to the lower proton Fermi energy in Tc compared to Rh. In Tc we see a low-lying $5/2^+$ state. Any $K-2$ satellite band may be spoiled by excessive mixing of $K=1/2$ and 3/2 components.

Also of interest is the identification of the $\pi 1/2^+[431]$ intruder band, band 5, in ^{107}Tc. Assignment of a configura-

TABLE IV. Determinations of total internal conversion coefficients and multipolarities of low-lying transitions in ^{105,107,109}Tc.

		^{105}Tc						
Transitions	α_{total}(expt)	α_{total}(theory)				α_{total}(expt)	Multipolarity	
(keV)	Ref. [15]	*E*1	*E*2	*M*1	*M*2	This work	Ref. [15]	This work
64.5	1.08(24)	0.48	6.24	0.99	15.6	1.13(10)	*M*1	*M*1(+*E*2)
85.6	0.22(6)	0.21	2.23	0.44	5.25	0.22(8)	*E*1	*E*1
129.2		0.06	0.50	0.14	1.15	0.26(9)	*M*1	*M*1+*E*2
157.0		0.04	0.25	0.08	0.58	0.09(4)		*M*1(+*E*2)
		^{107}Tc						
Transitions	α_{total}(expt)	α_{total}(theory)				α_{total}(expt)	Multipolarity	
(kev)	Ref. [8]	*E*1	*E*2	*M*1	*M*2	This work	Ref. [8]	This work
53	1.0(4)	0.79	11.7	1.65	30.7		*E*1	
65.8	1.35(7)	0.45	5.68	0.92	14.1	<1.06	*M*1+*E*2	*E*1
71.7	0.52(9)	0.35	4.18	0.72	10.1	0.65(8)	*D*(*M*1 or *E*1)	*M*1
83	0.42(28)	0.23	2.50	0.47	5.80		*M*1	
138.4		0.05	0.39	0.11	0.90	0.16(8)		*M*1(+*E*2)
159.6		0.03	0.23	0.08	0.54	0.09(2)		*M*1(+*E*2)
		^{109}Tc						
Transitions	α_{total}(expt)	α_{total}(theory)				α_{total}(expt)	Multipolarity	
(keV)	Other work		*E*2	*M*1	*M*2	This work	Other work	This work
69.4		0.37	4.52	0.78	11.9	0.80(9)		*M*1
137.3		0.05	0.44	0.12	0.96	0.19(9)		*M*1(+*E*2)

tion was not made for band 5 in Ref. [9]. As discussed above, the $\pi 1/2^+[431]$ rotational band is identified and assigned in ^{105}Tc in our work as well as in ^{107,111,113}Rh [5–7], and there is an obvious analogy of level patterns among band 5 of ^{107}Tc and the $\pi 1/2^+[431]$ bands of ^{105}Tc and ^{107,111,113}Rh. Therefore, band 5 of ^{107}Tc is reasonably assigned a $\pi 1/2^+[431]$ configuration originating from the $\pi(g_{7/2}/d_{5/2})$ subshells, which possess large prolate deformations. It should be noted that in comparison with the analogous intruder bands in ^{105}Tc and those in ^{107,111,113}Rh, band 5 in ^{107}Tc is surprisingly much more strongly populated (see the intensities indicated in Table II). However, all the intruder bands observed in these Tc and Rh isotopes show the common feature that the relative intensities of the bands decrease much more slowly with increasing excitation energies and spins than the normal bands. The intensity pattern may perhaps be accounted for by the lower state density and less rotational damping in the potential well corresponding to the larger prolate deformation possessed by the intruder orbital.

C. ^{109}Tc

Another significant extension and expansion of the level scheme are achieved in ^{109}Tc (see Fig. 4). The $\alpha=-1/2$ signature branch of band 1 is extended from the 1084.4-keV level $15/2^+$ reported in Ref. [9] up to the 3218.0-keV $(27/2^+)$ level so that the band crossing is observed. The $\alpha=+1/2$ branch of band 1 is extended from the 3439.4-keV $(29/2^+)$ up to 4200.8-keV $(33/2^+)$ level. New transitions of 564.7, 155.1, 601.3, 201.1, 464.1, and 221.5 keV were found to cross-link the signature partners of band 1.

Band 2 is extended from 2137.4-keV $(19/2^+)$ up to 2643.3-keV $(23/2^+)$ level. New 238.6- and 267.4-keV transitions were observed as linking transitions in band 2. A weak new decay-out transition of 1053.0 keV of band 2 is identified.

Band 6, consisting of only one level reported in Ref. [9], is expanded with the lowest members of signature partners observed. This progress is achieved thanks to the clarification of the confusing ambiguity in determination of the feeding point of the 426.5-keV decay-out transition of band 6. After intensive checks of coincidence relationships using the less-compressed cube an overlapping transition of 297.9 keV, which has almost the same energy as the 298.1-keV transition in band 1, is identified and found to belong to band 6. Based on coincidence relationship and relative intensities of the 297.9-keV and the 332.1-keV transitions, and the identification of the 630.1-keV crossover transition, the 426.5-keV decay-out transition is believed to feed the $9/2^+$ level of band 1, instead of the $11/2^+$ level. This conclusion is supported by the observations of the decay-out 563.9-keV and 460.4-keV transitions feeding the $7/2^+$ and

TABLE V. Rotational constants in the $K=1/2$ intruder band.

Nucleus	A(keV) This work	A(keV) This work	A(keV) Ref. [18]	A_1(keV) Ref. [18]
^{105}Tc	19.9	−25.4		
^{107}Tc	20.1	−28.5		
^{111}Rh	20.0	−33.7	19.6	−33.6
^{113}Rh	20.0	−26.8	20.0	−26.8

$11/2^+$ levels of band 1, respectively. The level systematics and decay pattern of band 6 of ^{109}Tc are now obviously similar to that in ^{107}Tc and those in ^{107,109,111,113}Rh.

No beta-decay data on gamma transitions have been reported for ^{109}Tc so far as we know. By gating on the 579.6- and 147.5-keV transitions in band 1, which is the only possible gate for ICC determinations for the 137.3-keV transition because of serious peak contaminations especially the 137.3- and 139.6-keV transitions overlapping each over, the ICC of the 137.3-keV transition was determined to be 0.19(9) based on the intensity balance between the 298.1- and 137.3-keV transitions as described above for ^{105}Tc and ^{107}Tc. Then gating on the 437.6- and 587.6-keV transitions the ICC of the 69.4-keV transition was determined to be 0.80(9). So the 69.4- and 137.3-keV transitions are found to be of $M1$ and $M1(+E2)$ character, respectively (see Table IV). The spin/parity assignments for the low-lying levels of band 1 in ^{109}Tc are thus made, $5/2^+$ being assigned to the lowest level observed. The assignments for the upper part of band 1 are made (and also supported) by the reasonable assumptions of rotational character and the analogy of level patterns in comparison to those of ^{105}Tc and ^{107}Tc. Since the 2137.4-keV level of band 2 is found to be deexcited by the 905.5-keV transition to the 1231.9-keV $17/2^+$ level of band 1 and by the very weak 1053.0-keV transition to the 1084.4-keV $15/2^+$ level of band 1, band 2 is most probably a positive parity band, and it is reasonable to assign $19/2^+$ to the 2137.3-keV level.

As for ^{105}Tc and ^{107}Tc, $7/2^+[413]$ is assigned to band 1 in ^{109}Tc. Like band 6 in ^{107}Tc, band 6 in ^{109}Tc built on the excited $11/2^+$ level and deexciting to the yrast band and predominantly feeding the $(9/2^+)_1$ level also provide evidence of triaxiality in ^{109}Tc, although this band is not well developed. The level pattern of band 2 in ^{109}Tc, very similar to band 2 in ^{107,113}Rh [5,7]. The $5/2^-[303]$, $3/2^-[301]$, or $1/2^+[431]$ bands are not observed in ^{109}Tc.

IV. ANALYSIS OF THE $K=1/2$ INTRUDER BANDS

As discussed in the preceding section, we see evidence of the $K=1/2$ intruder band coming down from the proton orbital $1/2^+[431]$ above the $Z=50$ major shell gap. In ^{105}Tc we see five members of the negative-signature partner and three members of the positive-signature partner. In ^{107}Tc we think we see six members of the negative-signature partner. To analyze the $K=1/2$ intruder bands of ^{105,107}Tc we use the notation in Eq. (4-61) of Bohr and Mottelson [17]:

$$E_I = E_0 + A\, I(I+1) + A_1(-1)^{I+1/2}(I+1/2)\ \delta(K,1/2).$$

Similar to the work of Kurpeta *et al.* [18] on beta decay into rhodium isotopes, we calculate the three unknown coefficients above using the three lowest known levels in the intruder band. (Actually, they made a fit with one degree of freedom for ^{111}Rh, where they knew the energies of four levels. Their notation for the rotational parameters is somewhat different; they use a_I for our A and A_{2K} for our A_1.) We recalculated also the rhodium cases using our best values of energies from Ref. [7]. Even though we know many higher levels of these bands, it is evident that the moment of inertia is increasing as one goes higher in the band, so that higher-order terms would be required for fitting. By subtracting the final state from the initial state in the above equation, the constant E_0 is eliminated, leaving two simultaneous equations for two transition energies. These are solved for the unknown rotational constants A and A_1. For three of the four nuclei treated, we use the 7/2-3/2 transition energy and the 5/2-3/2, and for the ^{107}Tc levels where one of the signature partners is unknown, so we used the 11/2-7/2 transition energy as the second transition. We noted a small difference in the constants derived for ^{105}Tc when the alternative two transitions were used and made a small correction to the ^{107}Tc rotational constants. Table V summarizes our values with those of Kurpeta *et al.* [18]. We also note Rücker [15] gives values for the $K=1/2$ band in ^{105}Tc of $A=19.59$ keV and $A_1=-25.07$ keV. These parameters differ slightly from our values, since Rücker made a best fit of five levels, including the $9/2^+$.

We note that rotational constant A is remarkably constant among the four nuclei, indicating that the deformation and degree of pairing are quite similar. The staggering coefficient A_1 is somewhat more negative for ^{111}Rh compared to ^{105,107}Tc and ^{113}Rh. The ratio A_1/A is usually designated as the decoupling constant a.

Rücker makes use of his measurement of 0.175 ns half-life for the 530.2-keV level in ^{105}Tc to calculate the quadrupole deformation parameter of the $K=1/2$ intruder band. He derives a value of $\beta=0.35(4)$ which corresponds to $\varepsilon=0.32$. Of course, the formulas he uses are for axially symmetric shapes. We have not yet fully explored in our model calculations the effect of triaxiality on energy level spacings and transition probabilities in $K=1/2$ bands.

V. LEVEL SYSTEMATICS AND BAND CROSSINGS OF THE Tc ISOTOPES

The systematics and evolution of the yrast positive parity bands in ^{103,105,107,109}Tc are shown in Fig. 5(a). An evolution from a weak-coupling scheme towards a strong-coupling scheme from ^{97}Tc to ^{105}Tc was reported in Ref. [13]. The higher-spin states observed in ^{105}Tc and the new data for ^{107}Tc and ^{109}Tc obtained in this work show more clearly the

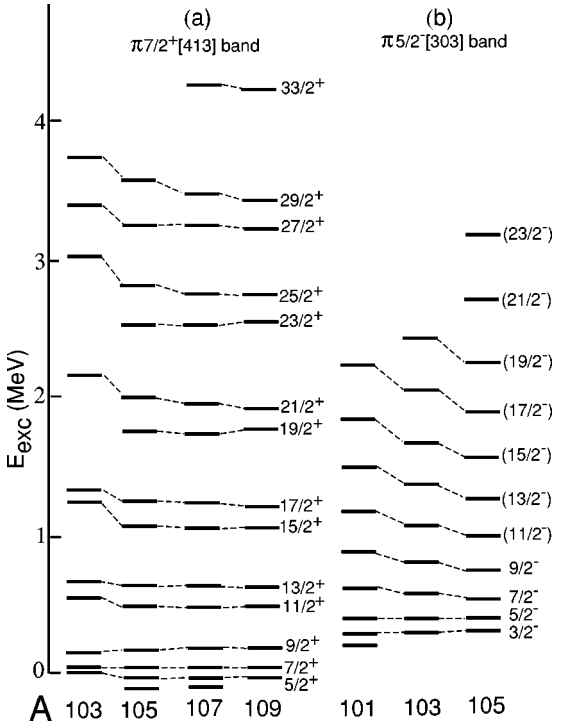

FIG. 5. Level systematics of the yrast positive- and negative-parity bands, $7/2^+[413]$ in ^{103,105,107,109}Tc (a) and $\pi 5/2^-[303]$ bands in ^{101,103,105}Tc (b). The $\pi 7/2^+[413]$ bands are adjusted to the $7/2^+$ level of ^{103}Tc, and the $\pi 5/2^-[303]$ bands to the $3/2^-$ level of ^{101}Tc. Data of ^{101,103}Tc are taken from Refs. [10,13].

strong-coupling scheme and the remaining large signature splitting in ^{105,107,109}Tc [see Figs. 5(a) and 6]. This evolution of coupling schemes can be interpreted as the changing of deformations. The proton Fermi level, being close to $1/2^+$ and $3/2^+$ of the $\pi g_{9/2}$ subshell for ^{97,99}Tc with small deformation, approaches the $5/2^+$ of the same subshell for $^{103-109}$Tc with larger deformations. In Fig. 5(a) it can also be seen that in the higher-spin states of the positive-parity bands of ^{105,107,109}Tc there is a tendency to deviate from the strong-coupling schemes when going to heavier isotopes, which may be interpreted again by the changing deformation: deformations may slightly become smaller with increasing neutron number for $N>62$ probably due to the neutron subshell at $N=64$.

The evolutions of negative-parity bands in ^{103,105}Tc are indicated in Fig. 5(b) for band 9 built on the intrinsic state $5/2^-[303]$. Smooth evolutions and similarities of the level patterns are seen in the figure. Large signature splitting in the $5/2^-[303]$ yrast negative-parity bands was reported in $^{97-99}$Tc [11–13], which was explained by the decoupling parameter of the $\pi 1/2^-[301]$ orbit from the $p_{1/2}$ subshell, $\alpha \sim 1$. However, almost no signature splitting in these bands is seen in the yrast negative-parity bands of ^{103,105}Tc [see Figs. 5(b) and 6]. We can draw no conclusions about possible triaxiality because no model calculations have been done for the more complicated odd-parity orbital system.

Level systematics of the $\pi 1/2^+[431]$ intruder bands of ^{105,107}Tc are shown in Fig. 7 together with that of $^{107-113}$Rh [5–7]. The smoothness and decreasing excitation energies

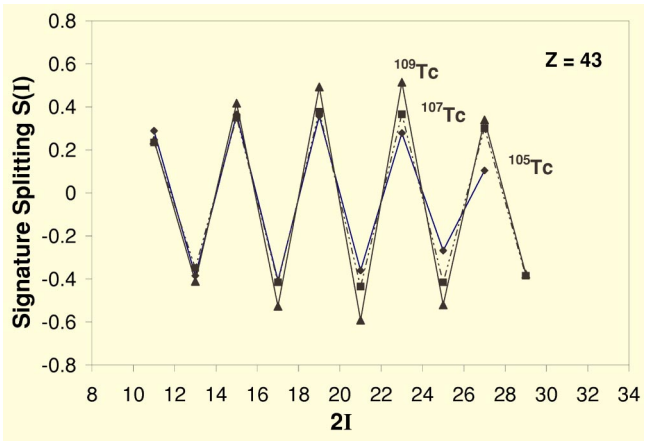

FIG. 6. Signature splitting of the yrast positive-parity bands in ^{105,107,109}Tc. ◆ represents ^{105}Tc, ■ is for ^{107}Tc, and ▲ is for ^{109}Tc.

with increasing neutron number in Tc isotopes are similar to those of isotones ^{107,109}Rh, although an opposite tendency is observed in the highest spin states in ^{111}Rh and possibly starting from the low levels in ^{113}Rh.

Indicated in Fig. 8 are the trends of band 6 of ^{105,107,109}Tc built on the excited $11/2^+$ states, with those of Rh isotopes also shown in the figure. As seen in Fig. 8, the lowering of excitations of the excited $11/2^+$ states when going to heavier isotopes is even more pronounced in Tc. As mentioned in the preceding section, the appearance of band 6 built on the excited $11/2^+$ state with rather low excitation energies, and

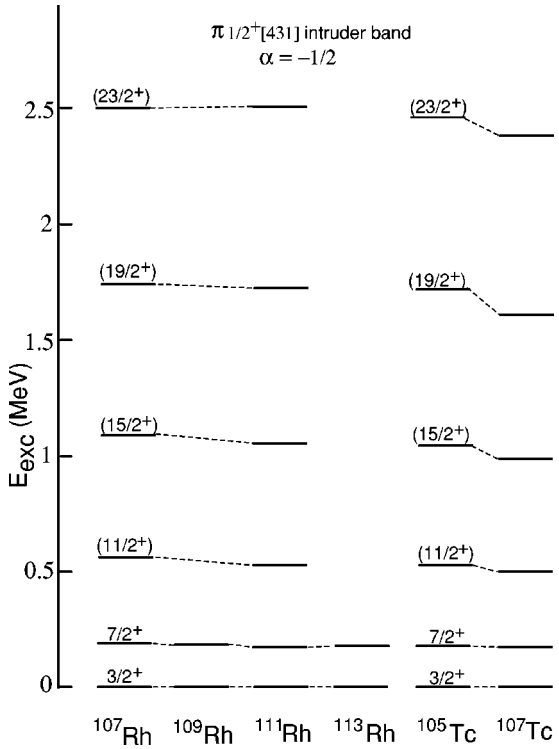

FIG. 7. Level systematics of the $\pi 1/2^+[431]$ intruder bands of ^{105,107}Tc. Also shown in the figure are those of ^{107,109,111,113}Rh [5,7]. The bands of Rh isotopes are adjusted to the $3/2^+$ level of ^{107}Rh, and that of ^{107}Tc to the $3/2^+$ of ^{105}Tc.

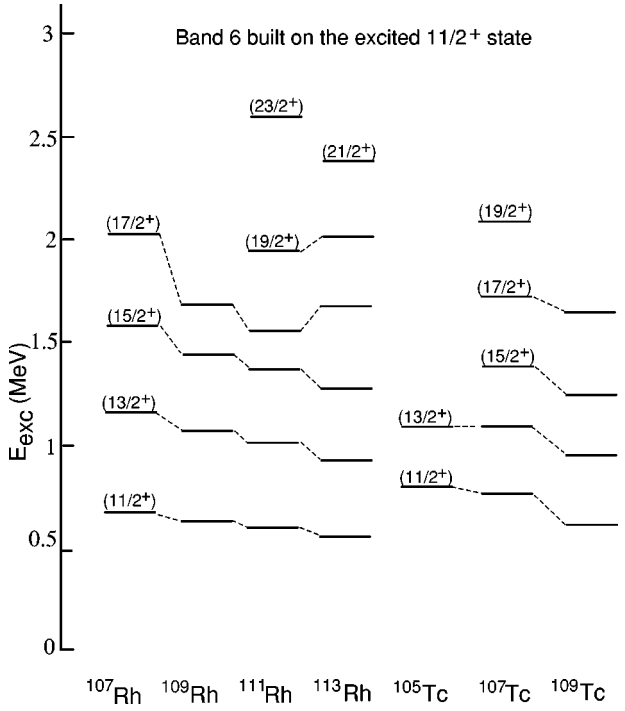

FIG. 8. Level systematics of the bands (band 6) built on the excited $11/2^+$ states in ^{105,107,109}Tc. Also shown in the figure are those of ^{107,109,111,113}Rh [5,7].

with a dominant decay feeding to the yrast $9/2^+$ state and very weak one to the yrast $7/2^+$ state of band 1, provides evidence of triaxiality.

The variations of the kinematic moment of inertia $J^{(1)}$ with rotational frequencies for the $\alpha=+1/2$ branch of the yrast positive parity bands of ^{105,107,109}Tc are shown in Fig. 9. It can be seen in Fig. 9 that the band-crossing frequencies of the $\alpha=+1/2$ branch of band 1 decrease with increasing neutron number, following the same trend as in ^{111,113}Rh [7]. In ^{109,111,113}Rh, the $\alpha=+1/2$ branch of band 1 exhibits band crossing at rotational frequencies $\hbar\omega\sim 0.38$, 0.37, and 0.35 MeV, respectively, with crossing frequencies decreasing with increasing neutron number [7]. It should also be noted that the $N=64$ (and $N=66$) isotones, ^{107}Tc and ^{109}Rh (and ^{109}Tc and ^{111}Rh), have almost the same band-crossing frequencies $\sim$0.38 MeV for ^{107}Tc and ^{109}Rh (and $\sim$0.37 MeV for ^{109}Tc and ^{111}Rh). Moreover, the corresponding band of odd-odd ^{112}Rh does not show any band crossing well past the rotational frequencies where the odd-even neighbors ^{109,111,113}Rh exhibit band crossings [7]. So, like the case of the Rh isotopes, the band crossings observed in ^{105,107,109}Tc are most likely related to the $h_{11/2}$ neutrons alignments. The high-spin parts of band 1 after band crossings have three-quasiparticle configurations with a broken pair of $h_{11/2}$ neutrons involved.

VI. TRIAXIAL-ROTOR-PLUS-PARTICLE CALCULATIONS

The rigid triaxial-rotor-plus-particle model was used in the paper of Luo *et al.* [7], where calculations based on this model were carried out for ^{111,113}Rh. The details of the model

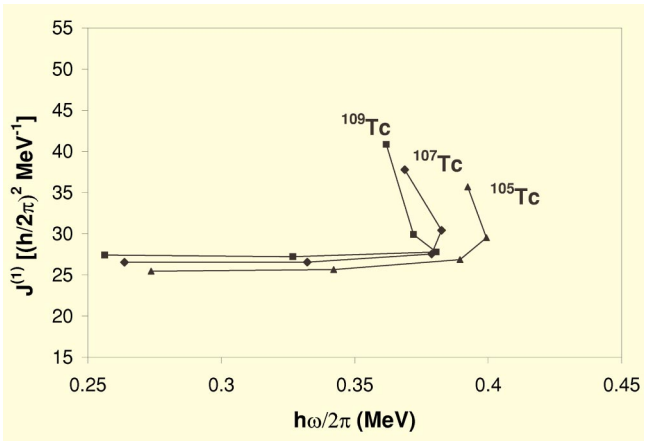

FIG. 9. Kinetic moments of inertia vs rotational frequencies of the $\alpha=+1/2$ member of band 1 in ^{105,107,109}Tc.

can be found Ref. [19] by Larsson *et al.* By "rigid" we mean that the shape, as defined by the deformation parameters, is the same for all states. We use the hydrodynamic irrotational flow formula for the ratios of the moments of inertia along the principal axes, which depend only on the deformation parameter γ. We normalize them with a scaling factor, which was fitted to the excitation energies. As a matter of fact, this is achieved by giving an effective value of $E(2^+)$ of the core. The single-particle Hamiltonian contains an anisotropic oscillator potential, which depends on the deformation parameters ε and γ. The quadrupole deformation parameter β may be related to parameter ε by Eq. (9) of Appendix H-4 of Ref. [8]. Only quadrupole deformation is considered; that is, we do not introduce hexadecapole or higher deformation parameters. We use the Lund convention for γ [20] for which the interval $0\geqslant\gamma\geqslant -60°$ corresponds to the collective rotation. Maximum triaxiality is achieved at $\gamma=-30°$.

In our work the model is employed to calculate the energies and wave functions of yrast and a few yrare states of ^{107}Tc. Several $E2$ and $M1$ transition strengths have also been calculated. Although the model program allows the use of variable moments of inertia, we used constant moments of inertia in order to reduce the number of free parameters. The fitting parameters then are ε, γ and $E(2^+)$. It is also possible to reduce the strength of the Coriolis force by an attenuation factor [21]. In the case of ^{107}Tc the fitted parameters are $\varepsilon=0.32$, $\gamma=-22.5°$, and $E(2^+)=0.35$ MeV. (To third order in ε the corresponding quadrupole deformation parameter β is then $\beta=0.38$.) A Coriolis attenuation parameter $\xi=0.8$ has been used throughout the calculation [7]. The parameter ξ was not a free parameter. Since the signature splitting function $S(I)$ is very sensitive to γ, its fit received special attention. The above shape is on the prolate side of maximum triaxiality. There is also a triaxial solution with γ on the oblate side, but it gives a poor fit for the yrare band.

The positive-parity bands in the investigated three isotopes are very similar, so that we can expect that ^{105,109}Tc have very similar structures. The comparison of the experimental and calculated yrast excitation energies is shown in Fig. 10. Above the $19/2^+$ level the comparison becomes irrelevant, because the model can describe only one quasipar-

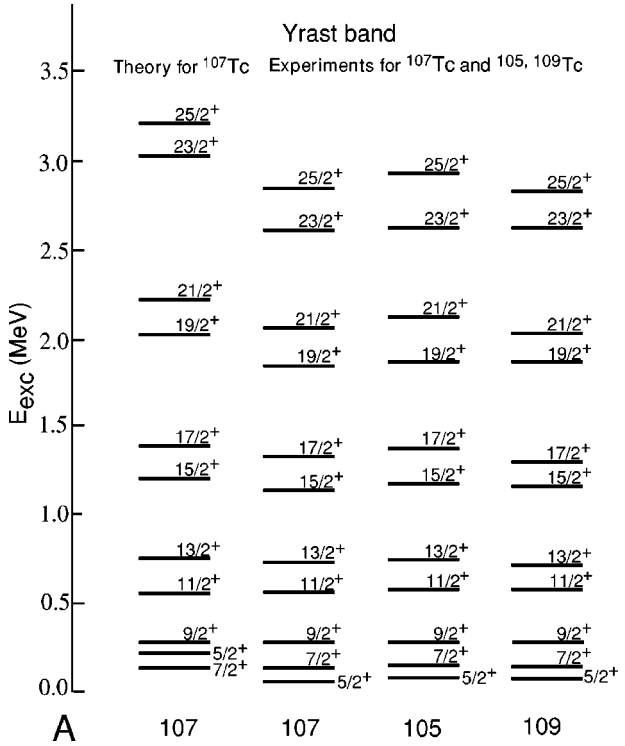

FIG. 10. Comparison of triaxial-rotor-plus-particle model calculations for the yrast band 1 of ^{107}Tc with experimental excitation energies of the bands in ^{105,107,109}Tc.

ticle coupled to a core. A similar behavior has been observed [7] in Rh. The backbending in ^{111,113}Rh has been attributed to an $h_{11/2}$ neutron pair alignment. As discussed in the preceding section, this seems to be the likely explanation for ^{105,107,109}Tc too. The most obvious disagreement of the model calculation with experiment is the position of the $5/2^+$ state, which lies below the $7/2^+_1$ state. In the calculation it has an excitation energy E_x=32.7 keV, while the lowest state of the yrast band is the $7/2^+$. As a matter of fact, the relation of the $5/2^+$ state to band 1 is not clear. A Harris plot [22] of the favored-signature band starting from $9/2^+$ was carried out. The two Harris parameters were fitted to the 9/2, 13/2, 17/2 states. The $5/2^+$ state clearly deviates from the extrapolated plot, thus suggesting that its intrinsic structure may be different from the rest of the ground band. In our calculation, the $5/2^+$ state is dominated by a component with K=5/2.

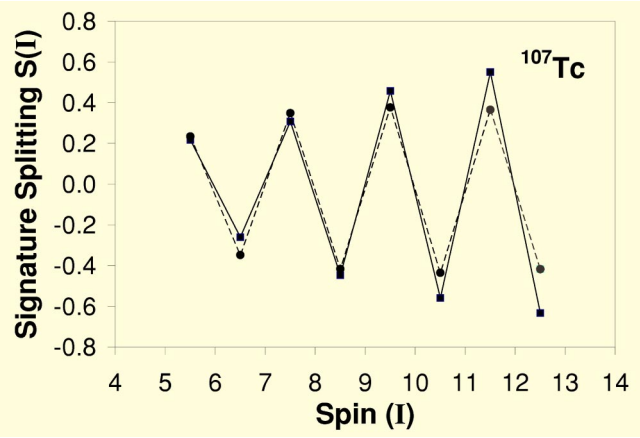

FIG. 11. Signature-splitting function comparison between theory and experiment for band 1 in ^{107}Tc. Experiment, dashed line; triaxial theory, solid line.

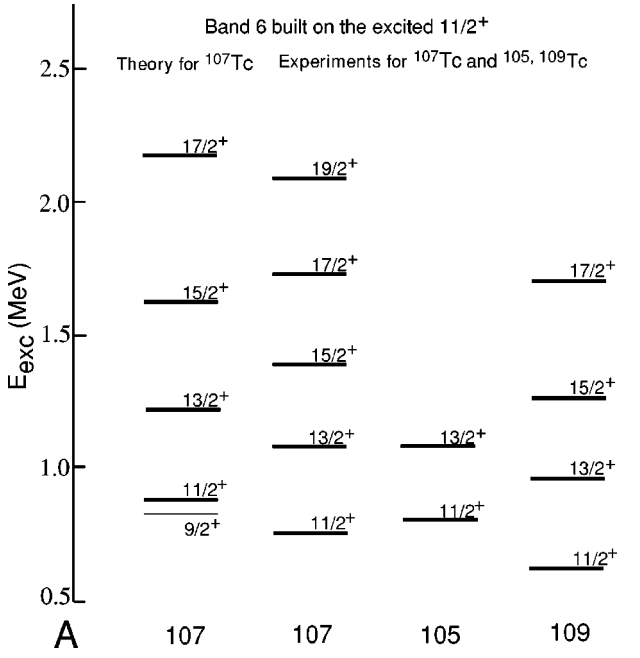

FIG. 12. Comparison of triaxial-rotor-plus-particle model calculation for band 6 built on the excited $11/2^+$ state of ^{107}Tc with experimental excitation energies of the bands in ^{105,107,109}Tc.

The model reproduction for the signature splitting functions of the positive parity yrast band of ^{107}Tc is illustrated in Fig. 11. The agreement between theory and experiment can be clearly seen.

The calculated excitation energies in band 6 are shown in Fig. 12. As discussed above, the sideband based on an $11/2^+$ state moves downwards when going from ^{105}Tc to ^{107}Tc and ^{109}Tc. The states belonging to this band have a wave function dominated by K=11/2, with a strong K=9/2 component. The calculation for ^{107}Tc also predicts a $9/2^+$ state located at ~60 keV below the 11/2 state. It is dominated by components with K=9/2. Even if this state exists, it will hardly be populated, so that a further discussion would be meaningless. This sideband has interesting properties. As mentioned in the previous sections, we first notice that the $11/2^+$ state decays mainly to the $9/2^+$ state of the ground band, while the intensity of the $11/2 \rightarrow 7/2$ transition is nearly an order of magnitude smaller. The explanation can be found if we look at the core wave functions of these three states. The dominant

TABLE VI. Gamma-ray branching ratios in ^{107}Tc.

Intensity Ratio	Theory	Expt.
$I(11/2 \rightarrow 9/2)/I(11/2 \rightarrow 7/2)$	2.2	6.6
$I(13/2 \rightarrow 11/2)/I(13/2 \rightarrow 9/2)$	0.47	0.74
$I(15/2 \rightarrow 13/2)/I(15/2 \rightarrow 11/2)$	0.91	3.9
$I(11/2_2 \rightarrow 9/2)/I(11/2_2 \rightarrow 7/2)$	8.0	7.3

TABLE VII. Model calculation: Energies and other properties of states.

E (keV)	2I	2K	$\langle J_z\rangle$	$\langle J_y^2\rangle$	$\langle J_x^2\rangle$	$\langle J_z^2\rangle$	$\langle \mathrm{I}\cdot\mathrm{j}\rangle/\lvert\mathrm{I}\rvert$	$\langle R_y^2\rangle$	$\langle R_x^2\rangle$	$\langle R_z^2\rangle$	$\langle \mathrm{R}\cdot\mathrm{j}\rangle/\lvert R\rvert$
0	7	7	−0.96	6.88	7.66	9.04	3.71	4.28	5.34	0.25	−2.82
32.7	3	1	0.43	6.47	5.43	0.35	1.73	3.94	5.21	0.16	−2.92
77.3	5	5	2.09	7.69	9.71	5.61	2.71	6.37	8.97	0.35	−3.78
142.7	9	7	−0.48	6.92	8.22	8.31	3.79	3.88	6.27	0.32	−1.42
212.6	7	1	0.34	7.3	5.14	0.46	2.12	3.93	7.62	0.25	−1.3
223.6	1	1	0.48	5.23	5.58	0.33	-0.57	6.19	6.59	0.1	−3.24
431.3	11	7	−0.57	7.11	7.69	8.8	3.57	6.57	9.72	0.36	−0.55
473.1	7	5	−0.64	7.15	8	8.2	2.03	8.05	14.26	0.65	−3.19
496.8	5	1	0.19	6.03	6.72	4.47	2.02	4.43	7.21	2.37	−3
511.7	5	1	0.16	5.64	8.52	2.96	1.61	4.1	10.01	2.21	−3.05
520.7	1	1	1.95	5.59	11.68	4.94	2.32	5.03	10.68	3.24	−4.64
539.7	3	3	−0.9	6.57	7.63	8.87	3.16	5.03	5.88	3.67	−4.44
624.3	13	5	−0.16	6.17	9.78	7.18	3.76	4.9	13.56	0.89	0.71
691.5	11	1	0.3	7.37	5.24	0.53	2.21	6.6	15.57	0.35	0.01
692.5	9	9	0.15	7.6	8.46	7.2	2.4	6.01	16.15	1.97	−2.3
753.1	11	11	−1.02	7.42	7.04	9.34	3.72	3.75	7.03	4.24	−0.4
766.9	3	3	0.43	5.45	6.66	0.67	0.11	5.25	7.12	3.74	−3.13
843.7	9	3	0.35	7.86	5.29	0.91	1.75	3.91	14.48	3.05	−1.16
1062.6	11	3	−0.88	8.19	7.24	8.12	2.61	6.7	18.8	2.6	−1.5
1076	15	5	−0.49	6.76	8.04	8.76	3.43	8.27	22.93	1.32	0.67
1083.6	13	11	−0.61	7.93	6.72	9.23	3.82	6.27	9.1	3.95	0.63
1263.9	17	5	−0.03	5.43	11.05	6.38	3.78	5.78	28.29	1.56	1.86
1369	13	7	−1.41	7.15	7.67	7.52	2.46	8.23	26.64	1.81	−0.85
1391.7	15	1	0.3	6.84	5.71	0.58	2.15	8.42	33.16	0.94	0.62
1500.3	15	9	−0.27	8.5	6.89	8.25	3.69	8.22	16.5	3.71	1.1
1558.4	1	1	−0.23	7.86	4.19	1.21	0.13	8.49	3.61	1.69	−3.54
1891.9	19	5	−0.39	6.72	8.15	8.7	3.33	9.84	44.91	1.96	1.29
2043.5	17	9	−0.3	9.12	6.11	8.66	3.31	11.59	30.11	3.44	0.87
2081.2	21	5	0.04	4.9	12.04	5.73	3.81	7.17	50.43	2.08	2.49
2162.1	17	11	−1.5	6.47	8.35	8.16	2.98	13.09	34.5	2.65	0.53
2254	19	1	0.31	6.36	6.15	0.52	2.16	9.52	58.56	1.61	1.02
2890.4	23	5	−0.31	6.78	8.22	8.58	3.26	11.37	75.29	2.49	1.64
3054.3	21	7	−1.14	9.32	5.79	8.65	2.59	9.06	75.96	2.53	0.5
3081.3	25	5	0.06	4.5	12.81	5.2	3.84	8.78	80.21	2.57	2.86
3286.2	23	1	0.29	6.01	6.49	0.51	2.22	10.91	90.5	2.18	1.33
4072.6	27	5	−0.25	6.84	8.3	8.45	3.21	12.88	113.6	3.01	1.88
4180.1	25	7	−1.18	9.2	5.82	8.75	2.58	10.93	111.7	2.93	0.87
4265.5	29	5	0.07	4.2	13.42	4.77	3.86	10.49	117.8	3.06	3.1
5440	31	5	−0.2	6.89	8.39	8.31	3.18	14.43	159.7	3.54	2.04

components in both the $7/2$ and $11/2$ states have a core angular momentum $R=2$. This means that the $E2$ strength of the $11/2\rightarrow 7/2$ transition is mainly determined by the diagonal matrix element of the quadrupole operator, which is reduced due to triaxiality. For $\gamma=-30°$ this matrix element simply vanishes. On the contrary, the core wave function of the $9/2^+$ state is dominated by $R=0$, so that the matrix element of the quadrupole operator can be large. This property is directly related to the triaxial deformation [23]. The calculated intensity ratio is $I(11/2\rightarrow 9/2)/I(11/2\rightarrow 7/2)=7.3$ (see Table VI), while the experimental value is 8.0. This is a simplified qualitative explanation. If we look at the core wave functions of yrare states, we notice also contributions from the core $K+2$ satellite band.

Another interesting aspect can be noticed if we look at the particle wave functions. The intrinsic particle wave function of the $11/2$ band head of band 6 differs very little from that of the $7/2_1$ state, namely, it is a mixing of the $[413]\Omega=7/2$ and $[422]\Omega=5/2$ asymptotic wave functions. As far as the amplitudes of components with good K are concerned,

the $11/2^+$ state is dominated by a mixture of $K=11/2$ and $9/2$, while the main components of the lowest $7/2^+$ state are $K=7/2$ and $5/2$. We remind the reader that Ω is the projection of the particle angular momentum j on the quantization z axis, while K is the projection of the total angular momentum I. In a triaxially deformed nucleus, these two quantum numbers need not be equal. According to Larsson *et al.* [19], in each basis function $K-\Omega$ must be an even integer. This increase of $\langle K\rangle$ shows that part of the core angular momentum R has been transferred from the x axis, with the largest moment of inertia, to the z axis. This feature has been observed [7] in odd-A Rh too. This transfer of core angular momentum is considered to be the main reason for the appearance of wobbling bands [24]. So far wobbling motion has been found only in odd-A nuclei that display alignment. The question of the possible manifestation of wobbling motion in odd-A Rh and Tc should be studied separately.

The calculated γ-ray branching ratios in the yrast cascade of ^{107}Tc have been compared with the experiment. The agreement is not as good as in ^{111,113}Rh, but the main trends can be reproduced (Table VI).

Some expectation values of observables are shown in Table VII; it constitutes the final part of the diagonalization output for positive-parity states. It is instructive to have a look at some characteristic features. The first column contains the calculated excitation energies. The second and third columns contain $2I$ and $2K$, i.e., twice the spin and the dominant projection quantum number, respectively. The quantization axis is the z axis, as usual. The x axis has the intermediate length and, as deduced from the hydrodynamical model, it has the largest moment of inertia. At $\gamma=-30°$ the moments of inertia along the y and z axes are equal, while the one along the x axis is four times larger. This means that the rotational energy of the core has its minimum value if the projection of R on the x axis has its maximum value.

The fifth column contains the expectation value of the projection of the particle angular momentum $\langle\Omega\rangle$. The following four columns give the expectation values of its squared projections on the three axes and the particle alignment along the total angular momentum. They are followed by the expectation values of the squared core angular momenta along the three axes. The last column represents the alignment along the rotational angular momentum direction. We will not discuss at length the content of this table, but we want to examine a few properties.

For instance, we will have a look at the distribution of the projections of R for yrast states. In the case of the $13/2^+_1$ state, $\langle R_x^2\rangle=13.56$, while the corresponding expectation values of $\langle R_y^2\rangle$ and $\langle R_z^2\rangle$ are 4.9 and 0.89, respectively. If we examine a state with unfavored signature, e.g., $11/2^+_1$, we notice a similar distribution, but with a somewhat reduced dominance of R_x^2. If we now look at the $11/2$ state at 753.1 keV (calculated energy), we notice that some core angular momentum has been transferred to the z axis, as mentioned in the discussion of band 6.

Shown in Fig. 13 are the model calculations for the $1/2^+[431]$ intruder band of ^{107}Tc and the experimental levels of this band in ^{107}Tc and ^{105}Tc. It can be seen in the figure that except for the lowest two levels of the $\alpha=-1/2$ branch of the band, large discrepancies are found between theory and experiment. These discrepancies need further study, particularly of the admixture of $g_{7/2}$ and $d_{5/2}$ character in the states.

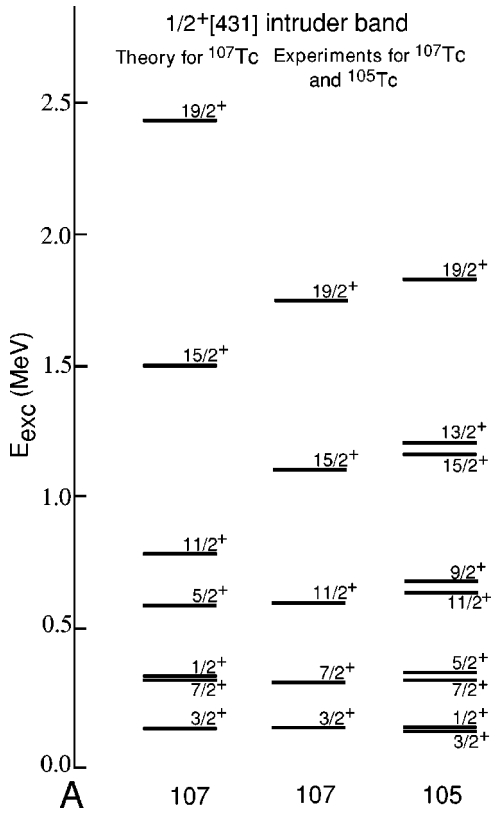

FIG. 13. Comparison of triaxial-rotor-plus-particle model calculation for the intruder band 5 of ^{107}Tc with experimental excitation energies of the bands in ^{105,107,109}Tc. Significant discrepancies between the theory and experiment can be seen.

VII. SUMMARY

Based on the high-statistics triple-coincidence data from Gammasphere, level schemes of ^{105,107,109}Tc are considerably extended and expanded. New level schemes are proposed and level systematics show trends in level patterns in this region of triaxial shape tendencies. Careful determinations of internal conversion coefficients (ICC) of low-lying low-energy transitions allow, or confirm, the spin/parity assignments of some low-lying levels. In the three Tc isotopes, bands with configurations of $\pi 7/2^+[413]$, $\pi 5/2^-[303]$, and $\pi 3/2^-[301]$ are identified, and $K=1/2$ $1/2^+[431]$ intruder bands are analyzed in terms of rotational constants. The band crossing of the yrast bands of the Tc isotopes are most likely related to $h_{11/2}$ neutron alignment. A principal feature, analogous to neighboring isotopes in Rh, is the appearance of a collective family of positive-parity bands. Triaxial-rotor-plus-particle model calculations are carried out and provide a basis for understanding the positive-parity bands. The model calculations gave the best fit to excitations, signature splittings, and branching ratios of the positive-parity bands of ^{107}Tc (and also in agreement with the experimental values of

^{105,109}Tc) at $\varepsilon = 0.32$ and $\gamma = -22.5°$ on prolate side of maximum triaxiality. The large discrepancies between the theory and experiment for the $K = 1/2$ intruder bands in the ^{105,107}Tc isotopes need further theoretical study.

ACKNOWLEDGMENTS

The work at Vanderbilt University, Lawrence Berkeley National Laboratory, Lawrence Livermore National Laboratory, and Idaho National Engineering and Environmental Laboratory are supported by U.S. Department of Energy under Grant No. DE-FG05-88ER40407 and Contract Nos. W-7405-ENG48, DE-AC03-76SF00098, and DE-AC07-99ID13727. The work at Tsinghua University in Beijing is supported by the Major State Basic Research Development Program under Contract No. G2000077400 and the Chinese National Natural Science Foundation under Grant No. 19775028. The Joint Institute for Heavy Ion Research is supported by its members, University of Tennessee, Vanderbilt, and the U.S. DOE. The authors are indebted for the use of ^{252}Cf to the office of Basic Energy Sciences, U.S. Department of Energy, through the transplutonium element production facilities at the Oak Ridge National Laboratory. Dr. Augusto Macchiavelli provided valuable help in setting up the Gammasphere electronics for data taking. Dr. Ken Gregorich was instrumental in design of the source mounting and plastic absorber ball and in mounting the source. The authors would also like to acknowledge the essential help of I. Ahmad, J. Greene, and R.V.F. Janssens in preparing and lending the ^{252}Cf source we used in the year 2000 runs. We greatly appreciate Dr. David Radford's developing and providing the new less-compressed RADWARE cube programs. The authors would like to thank Professor I. Ragnarsson and Professor P. Semmes for kindly providing the computer codes and for stimulating discussions. Ms. I. Stefanescu's valuable help is acknowledged with thanks.

[1] J. Skalski, S. Mizutori, and W. Nazarewicz, Nucl. Phys. **A617**, 282 (1997).
[2] J. H. Hamilton, in *Treatise on Heavy-Ion Science*, edited by Allan Bromley (Plenum, New York, 1989), Vol. 8, p. 2.
[3] J. H. Hamilton *et al.*, Prog. Part. Nucl. Phys. **35**, 635 (1995).
[4] H. Hua, C. Y. Wu, D. Cline, A. B. Hayes, R. Teng, R. M. Clark, P. Fallon, A. Goergen, A. O. Macchiavelli, and K. Vetter, Phys. Rev. C **69**, 014317 (2004).
[5] Ts. Venkova *et al.*, Eur. Phys. J. A **6**, 405 (1999).
[6] Ts. Venkova *et al.*, Eur. Phys. J. A **15**, 429 (2002).
[7] Y. X. Luo *et al.*, Phys. Rev. C **69**, 024315 (2004).
[8] *Table of Isotopes*, 8th ed., edited by R. B. Firestone and V. S. Shirley (Wiley, New York, 1996). For ^{107}Tc see H. Ohm *et al.*, Jülich Special Report No. 344 (1986), p. 30.
[9] J. K. Hwang *et al.*, Phys. Rev. C **57**, 2250 (1997).
[10] F. Hoellinger *et al.*, Eur. Phys. J. A **4**, 319 (1999).
[11] H. Aslan, B. Crowe, T. Dague, D. G. Savage, S. Zeghib, F. A. Rickey, and P. C. Simms, Phys. Rev. C **54**, 576 (1996).
[12] B. Crowe, H. Aslan, T. Dague, D. G. Savage, S. Zeghib, F. A. Rickey, and P. C. Simms, Phys. Rev. C **57**, 590 (1998).
[13] A. Bauchet *et al.*, Eur. Phys. J. A **10**, 145 (2001).
[14] D. C. Radford, Nucl. Instrum. Methods Phys. Res. A **361**, 297 (1995).
[15] M. Rücker, Ph.D. thesis, Johannes Gutenberg Univ., Mainz, Germany (1989).
[16] G. Lhersonneau *et al.*, Eur. Phys. J. A **1**, 285 (1998).
[17] A. Bohr and B. R. Mottelson, *Nuclear Structure* (Benjamin, New York, 1975), Vol. 2, p. 33.
[18] J. Kurpeta *et al.*, Eur. Phys. J. A **13**, 449 (2002).
[19] Larsson, G. Leander, and I. Ragnarsson, Nucl. Phys. **A307**, 189 (1978).
[20] S. G. Nilsson and I. Ragnarsson, *Shapes and Shells in Nuclear Structure* (Cambridge University Press, Cambridge, 1995).
[21] P. Ring and P. Schuck, *The Nuclear Many-Body Problem* (Springer, New York, 1980).
[22] S. H. Harris, Phys. Rev. **138**, B509 (1965).
[23] I. Hamamoto and B. R. Mottelson, Phys. Lett. **132B**, 7 (1983).
[24] I. Hamamoto and G. Hagemann, Phys. Rev. C **67**, 014319 (2003).